NANO LETTERS

2008
Vol. 8, No. 4
1179-1186

Single-Cell Fluorescence Imaging Using Metal Plasmon-Coupled Probe 2: Single-Molecule Counting on Lifetime Image

Jian Zhang,[†] Yi Fu,[†] Dong Liang,[‡] Kazik Nowaczyk,[†] Richard Y. Zhao,[‡,§,||] and Joseph R. Lakowicz*[,†]

Center for Fluorescence Spectroscopy, University of Maryland School of Medicine, Department of Biochemistry and Molecular Biology, 725 West Lombard Street, Baltimore, Maryland 21201, Division of Molecular Pathology, Department of Pathology, Department of Microbiology-Immunology, Institute of Human Virology, University of Maryland School of Medicine, 10 South Pine Street, Baltimore, Maryland 21201

Received January 11, 2008; Revised Manuscript Received February 21, 2008

ABSTRACT

Multiple Alexa Fluor 647-conjugated concanavalin A (conA) molecules were covalently bound to a single 20 nm silver particle to synthesize metal plasmon-coupled probes (PCPs). The fluorescence images were recorded by scanning confocal microscopy in both intensity and lifetime. The brightness of PCPs was 30-fold brighter than those of free conA and the lifetime of PCPs was shortened dramatically. PCPs were used to label T-lymphocytic (*PM1*) cells. The emission spots by PCPs bound on the cell surfaces were separated clearly from the cell images by autofluorescence due to the brighter signal and shorter lifetime of PCPs. The emission spots by PCPs were also scanned in three dimensions to count the distribution of bound fluorophores on the cell surfaces. The metal-associated fluorophores thus are suggested using as novel molecular imaging agents to quantify the components and describe their distributions on the cell surfaces.

Molecular fluorescent imaging techniques show great promise for elucidating signaling pathways and performing disease diagnosis at a single molecular level when they are targeted to bind on the cell surface.[1,2] An imaging agent consists of an fluorophore moiety and a targeting functionality, e.g., an antibody, peptide, DNA, or a special ligand.[3,4] Organic dyes are usually used in the most agents. However, these organic fluorophores cannot satisfy the requirements to the agents due to their disadvantages, e.g., low signal/baground ratio, poor photostability, and strong photoblinking. Moreover, the lifetime images sometimes are more important than the intensity images, but the lifetimes of most organic fluorophores are in the range of 2–4 ns, close to the value of cell autofluorescence.[5] This result will influence the identification of emission by fluorophores from background autofluorescence. Thus, it is of importance to develop novel molecular imaging agents that have brighter emission signal, different lifetime, more photostability, and less photoblinking.

Metal-enhanced Raman scattering was first reported 20 years ago.[6,7] Ten years ago, the study on metal-enhanced fluorescence (MEF) appeared.[8] Since then, many works have been done on theory and experiment.[9–15] A fluorophore can be described as an oscillating dipole used to radiate energy in emitting while a metal particle displays a plasmon resonance by electron oscillation on its surface.[16] When localizing a fluorophore near a metal particle, the radiating energy of fluorophore is altered dramatically via a near-field interaction with the metal particle. As a result, the fluorescence is enhanced significantly. Because this fluorescence enhancement occurs through an apparent increase of the intrinsic decay rate, the lifetime of fluorophore is shortened dramatically.

Most MEF results are reported on the metal films, but to our knowledge, there are still some publications from us and other laboratories that describe the occurrence of MEF on single metal particles.[8a,17–19] We think that the fluorescence behavior of an excited fluorophore on the metal particle, e.g.,

* Corresponding author. E-mail: Lakowicz@cfs.umbi.umd.edu.
[†] Center for Fluorescence Spectroscopy, University of Maryland School of Medicine, Department of Biochemistry and Molecular Biology.
[‡] Division of Molecular Pathology, Department of Pathology, University of Maryland School of Medicine.
[§] Department of Microbiology-Immunology, University of Maryland School of Medicine.
[||] Institute of Human Virology, University of Maryland School of Medicine.

10.1021/nl080093z CCC: $40.75
Published on Web 03/15/2008

Scheme 1. Tiopronin-Coated Silver Particles were Succinimidylated by Succinimidyl Ester-Terminated Thiolate Compound via Ligand Exchange and Covalently Bound by Alexa Fluor 647 conA Conjugates via Condensation

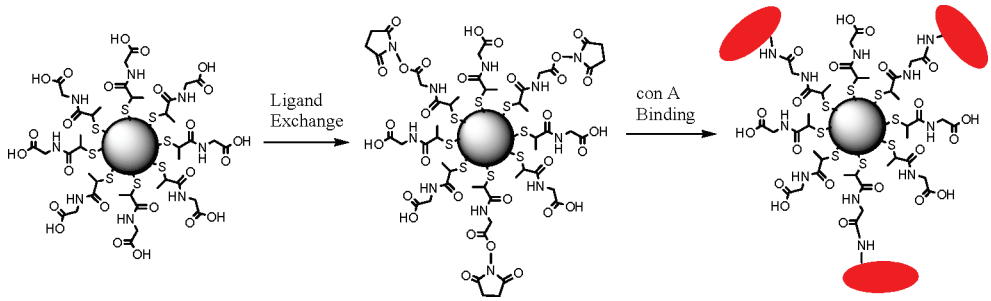

quenching or enhancement is principally dependent on the near field interaction, and the near field interaction comes from both factors of metal particle and fluorophore such as metal species of particle, size and shape of metal particle, distance from the fluorophore to the surface of metal core, and excitation and emission wavelengths of the fluorophore, etc. A small metal particle is shown to display a quenching effect to fluorescence, but a large metal particle can enhance fluorescence.[16a] Moreover, if the distance between the fluorophore and metal particle is too close, it can result in a quenching to fluorescence, but an optimistic distance can cause an enhancement. Besides the experimental results, some theoretical calculations have been reported recently confirming this viewpoint.[20]

We also observed the photostability of the fluorophore is extended and the photoblinking is reduced when the fluorophore is optimistically localized on the metal particle.[16] In addition, the versatile surface reactions on the metal particle can help us to bind the functionalities on them.[21] Thus, we suggest developing the metal-associated fluorophores as novel molecule-imaging agents in the cell labeling. Because MEF occurs via the interaction of the fluorophore with the metal plasmon resonance, the metal-associated fluorophores are also defined as metal plasmon-coupled probes (PCPs). In this study, the functionalized PCPs were synthesized using 20 nm silver particles. Because of a weak quenching by the silver particles, we used the silver salt instead of the gold salt to synthesize the metal particles. Our previous results reveal that for the fluorophore attached on the metal particle, the MEF efficiency increases with the size of metal core to exhibit a maximum at 50 nm, and then decreases.[20a] The 20 nm silver particle thus shows a capability to induce an efficient MEF. Because of its relatively small size, the 20 nm silver particle also displays a low steric hindrance when binding on the cell surface. The silver particle is fluorescently labeled by a direct binding of the Alexa Fluor 647 concanavalin A (conA) conjugate molecules. The fluorophores on the labeled conA are separated from the surface of metal core by the bound conA molecules as well as a linker of ca. 1 nm length. Because the conA molecule has a diameter of 8 nm,[22] the fluorophores that are randomly distributed on the conA molecule are supposed to range from 1 to 9 nm through the space from the surface of metal core. The average distance thus is estimated to be ca. 4.5 nm, at which the fluorescence can be enhanced. Our previous research has turned out that the intensity enhancement is always accompanied by the lifetime shortening.[19] This behavior is important for the development of PCPs and for the lifetime imaging described in this study.

Recently, we reported the fluorescence images of cells externally labeled by PCPs on the cell surfaces.[23] Alexa Fluor 647 conA conjugates were covalently bound on 20 nm silver particles. However, the conA molecule was only bound on the 20 nm silver particle in the molar ratio of 1/1. We suggested binding the single metal particles with multiple conA molecules and the emission spots by the metal-associated fluorophores could become brighter on the cell images. However, one shortcoming of our prior study was that the lifetime images of cells were not tested. In addition, the cell surfaces were bound by saturated PCPs. As the consequences, no individual emission spots could be separated from each other. In this study, we used the same silver particles, which were coated with *N*-(2-mercaptopropionyl)glycine (abbreviated as tiopronin).[24] These water-soluble silver particles were shown to be chemically stable (Scheme 1). In the incumbent, the amount of PCPs was tightly controlled to ensure that only few metal-associated fluorophores were bound on the cell surfaces. Subsequently, the fluorescence images of *PM1* cells were recorded in the emission intensity and lifetime using scanning confocal microscopy. The collected data were analyzed and compared with those by free conA in the absence of metal. The potential enhancing effect of metal particles on the detection of conA was investigated.

Experimental Section. All reagents and spectroscopic grade solvents were used as received from Sigma-Aldrich. Alexa Fluor 647 labeled conA is commercially available from Molecule Probe. *PM1* cell line was obtained through the AIDS Research and Reference Reagent Program, the National Institutes of Health. RC dialysis membrane (MWCO 50000) was purchased from Spectrum Laboratories, Inc. Nanopure water (>18.0 MΩ cm^{-1}), purified using Millipore Milli-Q gradient system, was used in all experiments. (2-Mercapto-propionylamino) acetic acid 2,5-dioxo-pyrrolidin-1-yl ester was synthesized as we reported previously.[25]

Preparation and Terminal Succinimidylation of a Tiopronin-Coated Silver Nanoparticle. Tiopronin-coated silver nanoparticles were prepared using a modified Brust reaction with a mole ratio of tiopronin/silver nitrate = 1/6 in methanol using excess amount of sodium borohydride as reducing agent.[21] These silver particles were succinimidylated via ligand exchange.[20] (2-Mercapto-propionylamino) acetic

acid 2,5-dioxo-pyrrolidin-1-yl ester (4×10^{-6} M) and silver particles (4×10^{-8} M) were codissolved in a mixing solvent of water/ethanol (v/v = 1/1) and stirred for 72 h at room temperature. The ligands displacements were expected to occur on the metal cores in a mole ratio of 1/1. Unbound compounds were removed by centrifuging at 6000 rpm for 30 min. The residuals were dispersed in 10 mM PBS buffer solution and then further purified by dialysis against 10 mM PBS buffer solution (MWCO 50000).

Binding Alexa Fluor 647 conA Conjugates on Silver Particles. Alexa Fluor 647 conA conjugates were covalently bound on the succinimidylated metal particles by condensation between succinimidyl ester moieties on metal particles and amino moieties on conA molecules.[26] The metal particle (2×10^{-8} M) and Alexa Fluor 647 conA conjugate (2×10^{-5} M) were codissolved in 10 mM PBS buffer solution at pH = 7.2 for 2 h. The impurities and aggregates of metal particles were removed from the reaction solution by centrifuging at 2000 rpm for 5 min. The solution was further centrifuged at 6000 rpm from 30 min to precipitate the metal particles. After removing the suspension, the residue was dispersed in 10 mM PBS solution. A drop of ammonium was added to terminate the residual succinimidyl ester moieties on the metal particles. The labeled metal particles were precipitated again by centrifuging at 6000 rpm, washed at least three times with buffer solution, and dispersed in 10 mM PBS solution.

Cell Culture. The T-lymphocytic *PM1* cell line, which is a colonial derivative of HUT78, was separated by Ficoll-Hypaque density gradient centrifugation. They were grown in the RPMI-1640 culture medium (Sigma) supplemented with 10% (v/v) heat-inactivated fetal bovine serum (Atlanta Biologicals Inc., GA) and contained 200 units/mL penicillin, 200 units/mL streptomycin (Invitrogene), and recombinant human interleukin (100U/mL) (Roche, Indianapolis, Indiana) for 6 days prior to fluorescent labeling. The number of cells was counted to be ca. 5×10^5 cells/mL.

Conjugating Free conA and conA-Bound Metal Particles on Cell Surfaces. *PM1* cells were suspended in 500 μL aliquots of 1 pM free conA in 10 mM PBS buffer solutions (pH = 7.2) for 1 h.[20] The conA-bound metal particles were incubated with the *PM1* cells in 500 μL aliquots of 0.03 pM conA-bound metal particles for the same incubation time as free conA. All cell samples were washed at least three times with PBS buffer solution before casting on the glass coverslips for fluorescence image measurements.

Spectra Measurements. Absorption spectra were monitored with a Hewlett-Packard 8453 spectrophotometer. Ensemble fluorescence spectra were recorded with a Cary Eclipse fluorescence spectrophotometer. Transmission electron micrographs (TEM) were taken with a side-entry Philips electron microscopy at 120 keV. Samples were cast from water solutions onto standard carbon-coated (200–300 Å) Formvar films on copper grids (200 meshes) by placing a droplet of a 10 times diluted aqueous sample solution on grids. The size distribution of metal core was analyzed with a Scion Image Beta Release 2 counting at least 200 particles.

All cell image measurements were performed using a time-resolved confocal microscope (MicroTime 200, PicoQuant).[27]

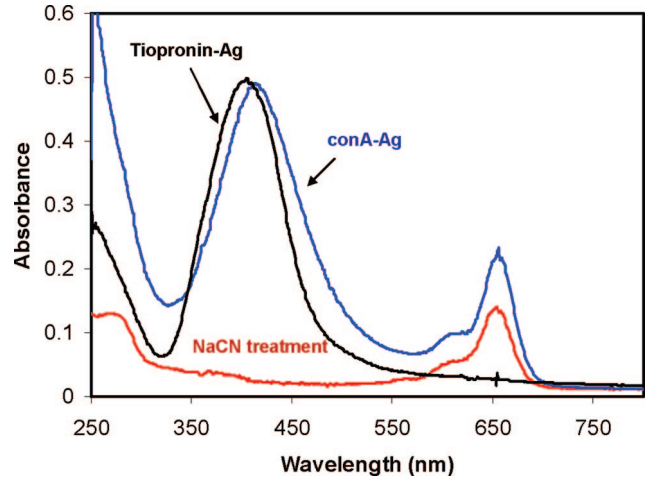

Figure 1. Absorbance spectra of tiopronin-coated silver particles, conA-bound metal particles, and released conA after the metal cores were dissolved by NaCN in 10 mM PBS buffer solution.

The samples were immobilized on glass coverslips by adding 20 μL of suspension onto an amino-silanized coverslip following by drying at room temperature. A single-mode pulsed laser diode (635 nm, 100 ps, 40 MHz) (PDL800, PicoQuant) was used as the excitation light. The collimated laser beam was spectrally filtered by an excitation filter (D637/10, Chroma) before directing into an inverted microscope (Olympus, IX 71). An oil immersion objective (Olympus, 100× , 1.3 NA) was used to focus laser light and collect fluorescence signal. The fluorescence that passed a dichroic mirror (Q655LP, Chroma) was focused onto a 75 μm pinhole for spatial filtering to reject out-of-focus signals and then reached the single-photon avalanche diode (SPAD) (SPCM-AQR-14, Perkin-Elmer Inc.). Images were recorded by raster scanning (in a bidirectional fashion) the sample of the incident laser with a pixel integration of 0.6 ms. The excitation power into the microscope was maintained at less than 1 μW. Time-dependent fluorescence data were collected with a dwell time of 50 ms. The data was stored in a time-tagged-time-resolved (TTTR) mode, which allows recording of every detected photon with its individual timing information. Instrument response function (IRF) widths of about 300 ps fwhm were obtained in combination with a pulsed diode laser, which permits the recording of subnanosecond fluorescence lifetimes extendable to less than 100 ps with reconvolution. Lifetimes were estimated by fitting to a χ_2 value of less than 1.2 and with a residuals trace that was fully symmetrical about the zero axis. All measurements were performed in a dark compartment at room temperature.

Results and Discussion. The synthesized tiopronin-coated silver particles displayed a typical plasmon absorbance at 402 nm in water (Figure 1).[19a,28,29] TEM images showed these metal particles appeared an approximately homogeneous distribution of metal core sizes and at least 80% were ranged in 20 ± 8 nm (inset of Figure 2). An average chemical composition thus was estimated to be (Ag)2 × 10^5 (Tio)5

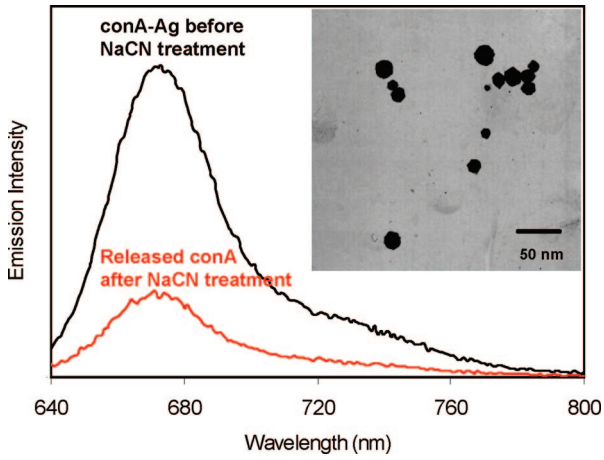

Figure 2. Ensemble fluorescence spectra of PCPs and released conA by NaCN treatment in 10 mM PBS buffer solution. The conA concentration remained unchanged. Inset represents typical transmission electron micrograph (TEM) images of 20 nm tiopronin-coated silver particles.

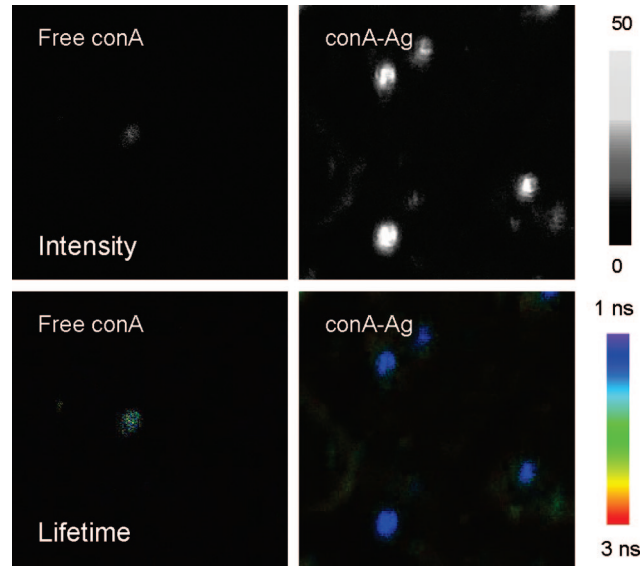

Figure 3. Representative emission intensity and lifetime images of (a) free conA in the absence of metal and (b) conA-bound metal particles. The images were acquired by a scanning confocal microscopy. The scales of diagrams are 5 μm $\times$ 5 μm. The resolution is 200 pixels $\times$ 200 pixels with an integration of 0.6 ms/pixel.

$\times$ 10^3. The metal particles were functionalized by reactions on the surfaces of metal cores.

They were first succinimidylated with (2-mercapto-propionylamino) acetic acid 2,5-dioxo-pyrrolidin-1-ylester via ligand exchange.[21] The ligand exchange on the metal particle is known to occur in a molar ratio of 1:1. In the experiment, the metal particles and succinimidyl-terminated thiolate compound were codissolved in water at a molar ratio of 1:100. We did not expect that the reaction could be completely efficient. In other words, only some of the succinimidyl-terminated ligands were expected to displace on the metal particle and the loading number of succinimidyl-terminated ligand should be less than 100 on each metal particle. It is difficult to measure the exact number using the regular evaluation methods, but the following experiments reveal that about 30 labeled conA molecules are conjugated on each metal particle, indicating that the metal particles are indeed displaced by multiple succinimidyl-terminated ligands with the loading number of 30–100.

Alexa Fluor 647 conA conjugates were covalently bound on the succinimidylated metal particles. In the reaction, conA was dissolved in solution by 1000 excess relative to the metal particle to avoid their aggregation. Because each metal particle is displaced by multiple succinimidyl-terminated ligands as described above, an excess amount of conA molecules were dissolved in solution ensuring at least 10 times more than the quantity of succinimidyl-terminated ligands on the silver particles. Binding of conA on the metal particle was verified by absorbance spectrum showing 6 nm red-shift of maximum wavelength to 408 nm (Figure 1). We did not measure the maximum concentration of conA in solution that can avoid the aggregation of metal particles in the current experiment, but the TEM images show that the metal particles are not aggregated significantly at this molar ratio. Comparing with free conA in the absence of metal, the bound conA exhibited an insignificant change of emission wavelength but an obvious intensity enhancement when the concentration remained the same (Figure 2). Several drops of 0.1 N sodium cyanide solution were added in solution to remove the metal cores and release the conA from the metal particles at the same concentration in solution.[30] This 3-fold enhancement of MEF is consistent with our previous observation on the metal particle with the same size.[19] The metal particles displayed only insignificant change on TEM images after the surface reactions, implying that they were not obviously altered.

The loading number of conA on the metal particles could be estimated by either ensemble absorbance or emission spectrum. On the absorbance spectrum (Figure 1), we inferred that the molar ratio of conA (absorbance coefficient $= 1.6 \times 10^6\ M^{-1}\ cm^{-1}$) over the metal particle (absorbance coefficient $= 1.5 \times 10^7\ M^{-1}\ cm^{-1}$) was about 30. This value seems plausible because the metal particles were first succinimidylated with a 100-fold amount of succinimidyl compound and then covalently bound with an excess amount of conA molecules. This number can be also measured by ensemble fluorescence spectrum. After dissolving the metal cores by NaCN treatment, the concentration of released conA molecules in solution was detected by the emission intensity, so the number was estimated to be 28, close to that inferred from absorbance spectrum.

Both the free conA and PCPs in buffer solution were cast on the glass coverslips and dried in air for the fluorescence image measurements. Because the samples were diluted sufficiently in solutions, most of the bright spots on the image were assumed to be single conA molecules or single PCPs (Figure 3). It was shown that the emission spots by PCPs were 30-fold brighter than those by free conA in the absence of metal, meanwhile the lifetime was shortened from 2.2 ns by free conA to 1.0 ns by PCPs, which is due to a dramatic change of radiating energy of fluorophore near a metal

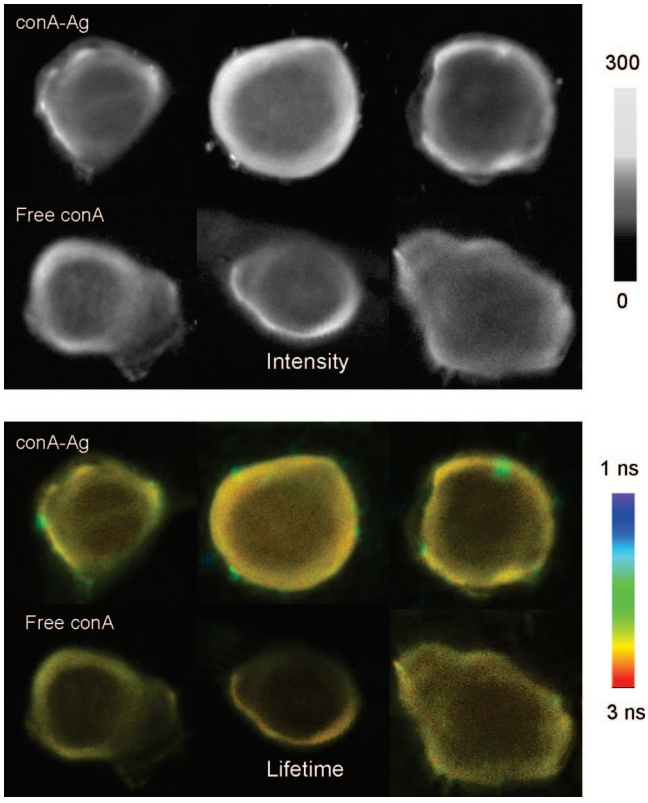

Figure 4. Representative emission intensity and lifetime images of *PM1* cells labeled by (a) conA in the absence of metal and (b) conA-bound metal particles. The scales of diagrams are 15 μm × 15 μm. The resolution is 400 pixels × 400 pixels with an integration of 0.6 ms/pixel.

particle.[17] The lifetime of free conA is found to be close to that of cell autofluorescence, but the lifetime of a metal-associated fluorophore is much shorter. With the brighter signal and shorter lifetime, the emission spots by PCPs are expected to be distinguished from the cell images by their autofluorescence when they are bound on the cell surfaces as the cell imaging agents.

In the current work, we want to count the number of fluorophores at the single-molecule level on the intensity or lifetime image of cell.[31,32] In the experiment, the *PM1* cells were fluorescently labeled with free conA and metal-associated fluorophores, respectively. In the two incumbents, the concentration of conA molecule was controlled to be the same in solution to make the collected cell images comparable. Both the intensity and lifetime images were recorded (Figure 4). However, although the emission spots could be observed on the intensity images labeled by either free conA or PCPs, it is not possible to tell whether they belong to heterogeneous medium of cell autofluorescence or fluorophores bound on the cell surfaces. This issue is solved on the lifetime images of cells when labeled by PCPs on which the emission spots by PCPs display significantly shorter lifetimes from the overall lifetime images of cells by autofluorescence (average about 2.5 ns). Moreover, these emission spots were also very bright as compared with the image background, 10-fold over the average intensity by the

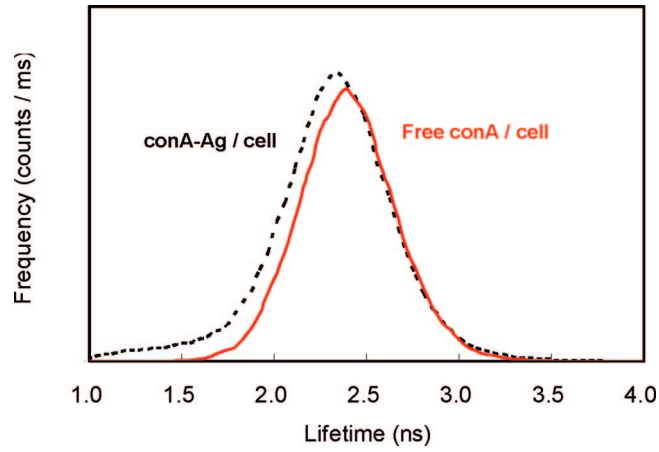

Figure 5. Histograms of lifetime distributions on the cells labeled by free conA and PCPs.

cell autofluorescence. This situation did not happen when free conA was used to label the cells.

The lifetime components on these emission spots were analyzed using the intensity decays and were achieved in two components as an average 2.5 and 1.2 ns, respectively. The longer component was considered to contribute from the autofluorescence of cell and the shorter component from PCPs bound on the cell surfaces. The mean average lifetime on these emission spots was estimated to be 1.7 ns, obviously shorter than the lifetime of cell autofluorescence. However, this value is also significantly longer than the unbound PCPs (Figure 3), probably due to the emission overlapping of bound fluorophores with the autofluorescence of cells. Contrary to PCPs, the emission spots by free conA could not be observed on either intensity or lifetime images. A histogram of lifetime distribution over the cell images by PCPs is presented in Figure 5. Although only a few PCPs were controlled to bind on the surface of each cell, their existence were still able to be observed by a slight rise near 1.3 ns. Meanwhile, the maximum of lifetime distribution was shown to shift slightly from 2.5 ns by the free conA in the absence of metal to 2.3 ns by PCPs. This result indicates that PCPs are very sensitive when used as the imaging agents to bind and count the target molecules on the cell surfaces.

In general, the cell images were recorded while tightly focusing the laser beam on the glass coverslip surface. To achieve the distribution of PCPs on the cell surfaces, the cell images were also monitored in the z direction. It was done by adjusting the laser focus away from the coverslip surface up to different layers of cells at every 1 μm (Figure 6a). It was shown that the cell images became blurred beyond 7 μm, indicating that the cell thickness was approximately 7 μm on the top of the coverslip. The emission spots were also altered with various focuses, reflecting their actual localizations on the cell surface. All cell lifetime images were finally combined into one image using OriginPro 70 software (Figure 6b). Only lifetime data ranging from 1.1 to 2.3 ns were shown in the combined image to block the background and cell autofluorescence to the most extent. About 12 emission dots were achieved with their lifetimes shorter than 2.3 ns. Apparently, these spots were not homogeneous on

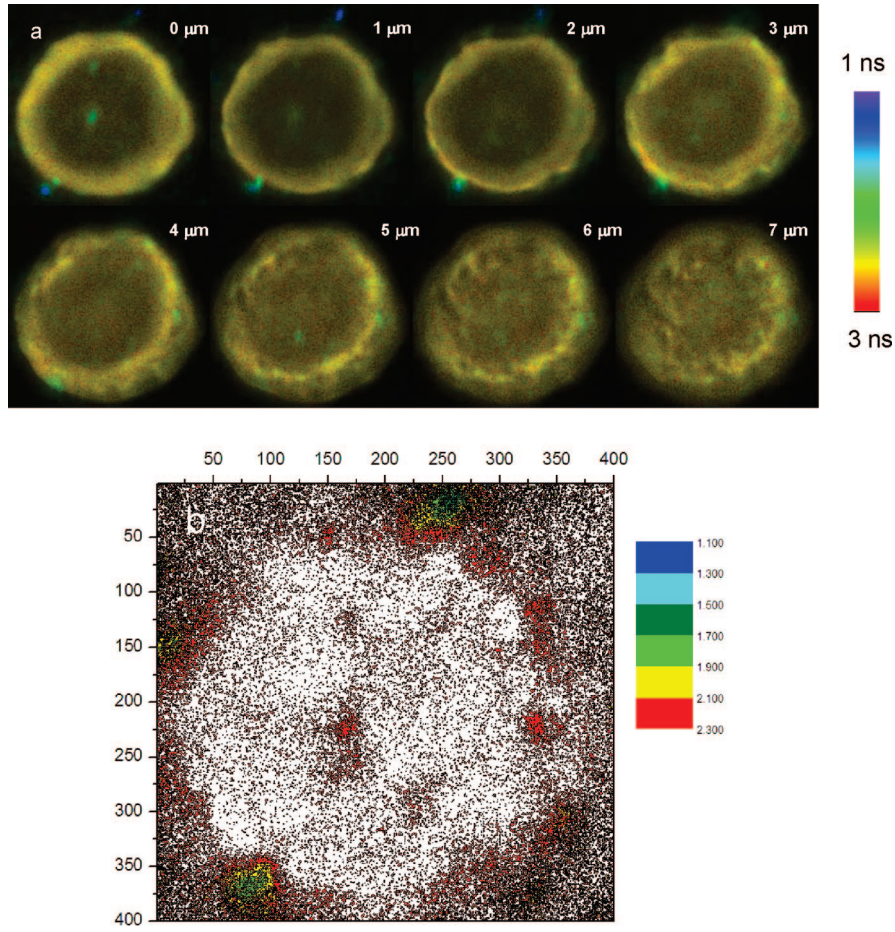

Figure 6. (a) Representative emission lifetime images of the same cell labeled by PCPs but scanned with a focus lifting from the top of coverslip to different layers of cell in a scale of 1 μm. The scales of diagrams are 15 μm $\times$ 15 μm. The resolution is 400 pixels $\times$ 400 pixels with an integration of 0.6 ms/pixel. (b) Combination of eight images in (a).

the sizes. We assume that small spots may represent single PCPs or small PCP clusters, while large spots may represent large PCPs clusters that are aggregated on the cell surface.

It is known that metal-enhanced fluorescence occurs via a near-field interaction of a fluorophore with a metal particle, which can be described as localizing the fluorophore in the electric field distributed near the metal particle.[33] The electric field distribution near the silver particle is an important element to understand the MEF behaviors of PCPs. Our experiments revealed that the efficiency increases with the size of metal core initially to exhibit a maximum at 50 nm and then decreases.[19a] The result fits well with the theoretical calculations by us[19a] and by others[20] using different models. Compared with the 20 nm silver particle, a larger silver particle of 50 nm is suggested to induce a more efficient MEF and a shorter lifetime due to a more efficient coupling effect with the fluorophore when conjugating the labeled conA molecules on the metal particle in the same loading number. However, we used solely the 20 nm silver particles to develop the functionalized PCPs in this case because larger PCPs may encounter stronger steric hindrance on the cell surfaces than the smaller ones. MEF is also influenced by the core shape of the metal particle. By theoretical calculation, a metal particle with rod, triangle, and core/shell structure is expected to have a totally different electric field distribution from a sphere near the metal core.[34,35] For instance, the electric field is specially concentrated at the ends for the metal rod and at the shape corners for the metal triangle. The efficiency of PCPs can be improved when the fluorophores are localized on these special sites of the shaped metal particles. The distance of fluorophore to the metal core also plays a crucial role.[16] An optimistic distance is important to influence the MEF efficiency. For instance, a distance that is too close can result in quenching and a distance that is too far cannot induce an efficient MEF. In this case, the distance is adjusted by conA molecule with an average distance of 4.5 nm. This distance can be further extended by increasing the linker length. The wavelength of an incident light can further influence the distribution of the electric field near the metal particle,[33] so the excitation and emission wavelengths is supposed to influence the occurrence of MEF for a fluorophore near a metal particle. On the basis of our experimental results, the fluorophore with a long wavelength can be enhanced efficiently on the metal substrate.[9b] This is one of the reasons why the Alexa Fluor 647 was used in this study.

The emission spots by the aggregated PCPs on the cell images were observed to be much brighter than those by the single PCPs. According to Schatz, et al., the electric field in the space between the coupled metal particles is more

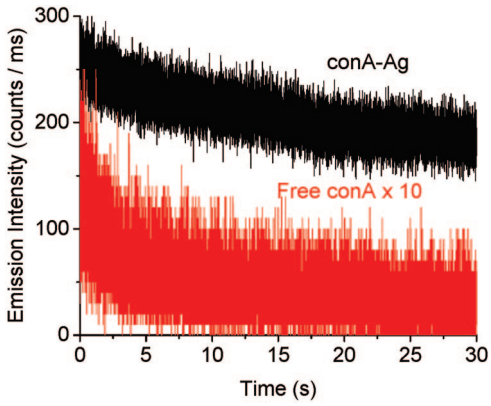

Figure 7. Respective time traces for single emission spots of free conA molecules in the absence of metal and metal-associated fluorophores.

intense than that of a monomer.[34,36] Our recent results have supported this viewpoint.[37] Therefore, besides the fluorescence overlapping by the aggregated metal particles associated on the cell surfaces, the strong near-field interactions to the fluorophores also affect the brightness of the emission spots on the cell images.

We also investigated the influence of metal particles on the photostability of bound fluorophores. A time trace of a free conA molecule showed direct decay of emission intensity with irradiation time until completely eliminated within 10 s (Figure 7). However, the emission intensity by a metal-associated fluorophore was reduced to 1/3 within 30 s, indicating that the photostability was lengthened 10-fold when conA was bound on the metal particle.[16]

Because the silver particles have been used as broad-spectrum antimicrobial agents,[38] we are concerned about the potential cytotoxicity of PCPs to *PM1* cells in culture. In fact, the cytotoxicity of silver particles is attributed to their surface chemistry.[39] If the silver particles possess nearly free surfaces, they could interact strongly with cells, resulting in cytotoxicity. However, in our study, the silver particle surfaces were coated with dense monolayers of thiolate amino acid ligands, which are known to be chemically stable in water. Moreover, the silver particles were bound on the surfaces of *PM1* cells through the conA molecules. Although we did not quantify cytotoxicity, no obvious cell death was detected when binding PCPs on the cell surfaces in our study.[40]

Conclusion. Alexa Fluor 647 conA conjugates were covalently bound onto 20 nm silver particles that were used as novel fluorescence imaging agents. The emission intensity and lifetime images of the fluorescently labeled *PM1* cells by PCPs were recorded by scanning confocal microscopy. As the results, the metal-associated fluorophores displayed a brighter signal, shorter lifetime, and better photostability than the free conA. The emission spots due to the PCP labels on the cell surfaces were clearly distinguishable from autofluorescence images of the cells by their brightness and lifetimes. Thus we can count the content and describe the distribution of target molecules on the cell surface when the metal-associated fluorophores are bound on the cell surfaces.

Acknowledgment. This research was supported by grants from NIH (HG-00255 and RR-08119 to J.R.L.) and research support from the University of Maryland Medical Center (R.Z.).

References

(1) Rosenthal, S. J.; Tomlinson, I.; Adkins, E. M.; Schroeter, S.; Adams, S.; Swafford, L.; McBride, J.; Wang, Y.; DeFelice, L. J.; Blakely, R. D. *J. Am. Chem. Soc.* **2002**, *124*, 4586.
(2) Chen, I.; Ting, A. Y. *Curr. Opin. Biotechnol.* **2005**, *16*, 35.
(3) Weissleder, R.; Tung, C. H.; Mahmood, U.; Bogdanov, A. *Nat. Biotechnol.* **1999**, *17*, 375.
(4) Ntziachristos, V.; Chance, B. *Breast Cancer Res.* **2001**, *3*, 41.
(5) Lakowicz, J. R. *Principles of Fluorescence Spectroscopy*, 3rd ed.; Kluwer Academic/Plenum Publishers: New York, 2006.
(6) Schatz, G. C. *Acc. Chem. Res.* **1984**, *17*, 370.
(7) Kerker, M. *Acc. Chem. Res.* **1984**, *17*, 271.
(8) (a) Sokolov, K.; Chumanov, G.; Cotton, T. M. *Anal. Chem.* **1998**, *70*, 3898. (b) Chumanov, G.; Sokolov, K.; Gregory, B. W.; Cotton, T. M. *J. Phys. Chem.* **1995**, *99*, 9466.
(9) (a) Shen, Y.; Swiatkiewicz, J.; Lin, T.-C.; Markowicz, P.; Prasad, P. N. *J. Phys. Chem. B* **2002**, *106*, 4040. (b) Zhang, J.; Matveeva, E.; Gryczynski, I.; Leonenko, Z.; Lakowicz, J. R. *J. Phys. Chem. B* **2005**, *109*, 7969.
(10) Antunes, P. A.; Constantino, C. J. L.; Aroca, R. F.; Duff, J. *Langmuir* **2001**, *17*, 2958.
(11) (a) Yu, F.; Persson, B.; Lofas, S.; Knoll, W. *J. Am. Chem. Soc.* **2004**, *126*, 8902. (b) Ekgasit, S.; Thammacharoen, C.; Yu, F.; Knoll, W. *Anal. Chem.* **2004**, *76*, 2210. (c) Baluschev, S.; Yu, F.; Miteva, T.; Ahl, S.; Yasuda, A.; Nelles, G.; Knoll, W.; Wegner, G. *Nano Lett.* **2005**, *5*, 2482.
(12) Lee, I.-Y. S.; Suzuki, H.; Ito, K.; Yasuda, Y. *J. Phys. Chem. B* **2004**, *108*, 19368.
(13) Song, J.-H.; Atay, T.; Shi, S.; Urabe, H.; Nurmikko, A. V. *Nano Lett.* **2005**, *5*, 1557.
(14) Kawasaki, M.; Mine, S. *J. Phys. Chem. B* **2005**, *109*, 17254.
(15) (a) Kumbhar, A. S.; Kinnan, M. K.; Chumanov, G. *J. Am. Chem. Soc.* **2005**, *127*, 12444. (b) Bruzzone, S.; Malvaldi, M.; Arrighini, G. P.; Guidotti, C. *J. Phys. Chem. B* **2005**, *109*, 3807.
(16) (a) Lakowicz, J. R. *Anal. Biochem.* **2005**, *337*, 171. (b) Lakowicz, J. R. *Anal. Biochem.* **2001**, *298*, 1.
(17) (a) Stoermer, R. L.; Keating, C. D. *J. Am. Chem. Soc.* **2006**, *128*, 13243. (b) Nicewarner-Pena, S. R.; Carado, A. J.; Shale, K. E.; Keating, C. D. *J. Phys. Chem. B* **2003**, *107*, 7360.
(18) (a) Chen, Y.; Munechika, K.; Ginger, D. S. *Nano Lett.* **2007**, *7*, 690. (b) Xie, F.; Baker, M. S.; Goldys, E. M. *Chem. Mater.* **2008**, http://dx.doi.org/10.1021/cm703121m.
(19) (a) Zhang, J.; Fu, Y.; Chowdhury, M. H.; Lakowicz, J. R. *J. Phys. Chem. C* **2008**, *112*, 18. (b) Zhang, J.; Malicka, J.; Gryczynski, I.; Leonenko, Z.; Lakowicz, J. R. *J. Phys. Chem. B* **2005**, *109*, 7643.
(20) Mertens, H.; Koenderink, A. F.; Polman, A. *Phys. Rev. B* **2007**, *76*, 115123.
(21) (a) Templeton, A. C.; Wuelfing, W. P.; Murray, R. W. *Acc. Chem. Res.* **2000**, *33*, 27. (b) Ingram, R. S.; Hostetler, M. J.; Murray, R. W. *J. Am. Chem. Soc.* **1997**, *119*, 9175.
(22) Yuan, F.; Dellian, M.; Fukumura, D.; Leunig, M.; Berk, D. A.; Torchilin, V. P.; Jain, R. K. *Cancer Res.* **1995**, *55*, 3752.
(23) Zhang, J.; Fu, Y.; Lakowicz, J. R. *Bioconjugate Chem.* **2007**, *18*, 800.
(24) Huang, T.; Murray, R. W. *Langmuir* **2002**, *18*, 7077.
(25) Zhang, J.; Roll, D.; Geddes, C. D.; Lakowicz, J. R. *J. Phys. Chem. B* **2004**, *108*, 12210.
(26) (a) Osella, D.; Pollone, P.; Ravera, M.; Salmain, M.; Jaouen, G. *Bioconjugate Chem.* **1999**, *10*, 607–612. (b) Kinter, A. L.; Poli, G.; Fox, L.; Hardy, E.; Fauci, A. S. *J. Immunol.* **1995**, *154*, 2448.
(27) (a) Fu, Y.; Lakowicz, J. R. *Anal. Chem.* **2006**, *78*, 6238. (b) Fu, Y.; Lakowicz, J. R. *J. Phys. Chem. B* **2006**, *110*, 22557.
(28) Kreibig, U.; Vollmer, M. *Optical Properties of Metal Clusters*; Springer Series in Materials Science, Vol. 25; Springer-Verlag: Berlin and Heidelberg, 1995.
(29) Hayat, M. A., Ed. *Colloidal Gold: Principles, Methods, and Applications*; Academic Press: San Diego, 1991.
(30) Rosi, N. L.; Mirkin, C. A. *Chem. Rev.* **2005**, *105*, 1547.
(31) Knemeyer, J.-P.; Herten, D.-P.; Sauer, M. *Anal. Chem.* **2003**, *75*, 2147.
(32) Rosenthal, S. J.; Tomlinson, I.; Adkins, E. M.; Schroeter, S.; Adams, S.; Swafford, L.; McBride, J.; Wang, Y.; DeFelice, L. J.; Blakely, R. D. *J. Am. Chem. Soc.* **2002**, *124*, 4586.

(33) Hao, E.; Schatz, G. C. *J. Chem. Phys.* **2004**, *120*, 357–366.
(34) (a) Kottmanna, J. P.; Martin, O. J. F.; Smithb, D. R.; Schultz, S. *Chem. Phys. Lett.* **2001**, *341*, 1. (b) Kottmann, J. P.; Martin, O. J. F.; Smith, D. R.; Schultz, S. *New J. Phys.* **2000**, *27*, 20–21.
(35) (a) Schelm, S.; Smith, G. B. *J. Phys. Chem. B* **2005**, *109*, 1689. (b) Wang, H.; Brandl, D. W.; Le, F.; Nordlander, P.; Halas, N. J. *Nano Lett.* **2006**, *6*, 827.
(36) (a) Kelly, K. L.; Coronado, E.; Zhao, L. L.; Schatz, G. C. *J. Phys. Chem. B* **2003**, *107*, 668. (c) Hao, E.; Li, S.; Bailey, R. C.; Zou, S.; Schatz, G. C.; Hupp, J. T. *J. Phys. Chem. B* **2004**, *108*, 1224.
(37) (a) Zhang, J.; Fu, Y.; Chowdhury, M. H.; Lakowicz, J. R. *Nano Lett.* **2007**, *7*, 2101–2107. (b) Zhang, J.; Fu, Y.; Lakowicz, J. R. *Langmuir* **2007**, *23*, 11734–11739.
(38) Efrima, S.; Bronk, B. V. *J. Phys. Chem. B* **1998**, *102*, 5947.
(39) Elechiguerra, J. L.; Burt, J. L.; Morones, J. R.; Camacho-Bragado, A.; Gao, X.; Lara, H. H.; Yacaman, M. J. *J. Nanobiotechnol.* **2005**, *3*, 1477.
(40) Poon, V. K.; Burd, A. *Burns* **2004**, *30*, 140.

NL080093Z